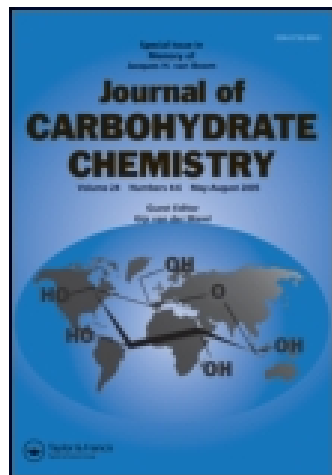


This article was downloaded by: [Pennsylvania State University]

On: 11 August 2014, At: 18:39

Publisher: Taylor & Francis

Informa Ltd Registered in England and Wales Registered Number: 1072954 Registered office: Mortimer House, 37-41 Mortimer Street, London W1T 3JH, UK



Journal of Carbohydrate Chemistry

Publication details, including instructions for authors and subscription information:

<http://www.tandfonline.com/loi/lcar20>

Fabrication and Thermal Property of Polyhedral Oligomeric Silsesquioxane (POSS)/Microcrystalline Cellulose (MCC) Hybrids

Hongxia Liu^{ab}, Xiaojian Li^c, Shiqi Wang^c, Shaojun Huang^c, Chun Wei^{abc} & Jian Lv^{abc}

^a Key Laboratory of New Processing Technology for Nonferrous Metals and Materials, Ministry of Education, Guilin University of Technology, Guilin 541004, China

^b Guangxi Scientific Experiment Center of Mining, Metallurgy and Environment, Guilin 541004, China

^c College of Material Science & Engineering, Guilin University of Technology, Guilin 541004, China

Published online: 12 Mar 2014.

To cite this article: Hongxia Liu, Xiaojian Li, Shiqi Wang, Shaojun Huang, Chun Wei & Jian Lv (2014) Fabrication and Thermal Property of Polyhedral Oligomeric Silsesquioxane (POSS)/Microcrystalline Cellulose (MCC) Hybrids, *Journal of Carbohydrate Chemistry*, 33:2, 86-103, DOI: [10.1080/07328303.2014.880115](https://doi.org/10.1080/07328303.2014.880115)

To link to this article: <http://dx.doi.org/10.1080/07328303.2014.880115>

PLEASE SCROLL DOWN FOR ARTICLE

Taylor & Francis makes every effort to ensure the accuracy of all the information (the "Content") contained in the publications on our platform. However, Taylor & Francis, our agents, and our licensors make no representations or warranties whatsoever as to the accuracy, completeness, or suitability for any purpose of the Content. Any opinions and views expressed in this publication are the opinions and views of the authors, and are not the views of or endorsed by Taylor & Francis. The accuracy of the Content should not be relied upon and should be independently verified with primary sources of information. Taylor and Francis shall not be liable for any losses, actions, claims, proceedings, demands, costs, expenses, damages, and other liabilities whatsoever or howsoever caused arising directly or indirectly in connection with, in relation to or arising out of the use of the Content.

This article may be used for research, teaching, and private study purposes. Any substantial or systematic reproduction, redistribution, reselling, loan, sub-licensing,

systematic supply, or distribution in any form to anyone is expressly forbidden. Terms & Conditions of access and use can be found at <http://www.tandfonline.com/page/terms-and-conditions>

Fabrication and Thermal Property of Polyhedral Oligomeric Silsesquioxane (POSS)/Microcrystalline Cellulose (MCC) Hybrids

Hongxia Liu,^{1,2} Xiaojian Li,³ Shiqi Wang,³ Shaojun Huang,³
Chun Wei,^{1,2,3} and Jian Lv^{1,2,3}

¹Key Laboratory of New Processing Technology for Nonferrous Metals and Materials, Ministry of Education, Guilin University of Technology, Guilin 541004, China

²Guangxi Scientific Experiment Center of Mining, Metallurgy and Environment, Guilin 541004, China

³College of Material Science & Engineering, Guilin University of Technology, Guilin 541004, China

Microcrystalline cellulose extracted from sisal fibers (SFMCC) and octa-aminopropyl polyhedral oligomeric silsesquioxane (POSS-NH₂) were used to fabricate POSS/SFMCC hybrids through a simple cross-linking process with epichlorohydrin as the cross-linking agent. The chemical structure and morphology of hybrids are characterized with FTIR spectra, X-ray diffraction, and SEM. The results present that POSS-NH₂ has been grafted onto the surface of SFMCC. The thermal property of hybrids has been improved with a 19°C higher maximum thermal decomposition temperature than SFMCC, as measured by TGA and DSC. The residual mass of hybrids and SFMCC were 15.6 wt% and 4.4wt% at 700°C, respectively.

Keywords Sisal fiber; Microcrystalline cellulose; POSS; Organic/inorganic hybrids; Thermal property

Received April 5, 2013; accepted December 30, 2013.

Address correspondence to Hongxia Liu, and Chun Wei, Key Laboratory of New Processing Technology for Nonferrous Metals and Materials, Ministry of Education, Guilin University of Technology, Guilin 541004, China. E-mail: aozihx@foxmail.com;1005668130@qq.com

Color versions of one or more of the figures in the article can be found online at www.tandfonline.com/lcar.

INTRODUCTION

Cellulose, the most abundant polymer on earth, is regarded as an almost inexhaustible source of raw materials. Cellulose solid particles including microcrystalline cellulose (MCC), cellulose microcrystals or nanowhiskers (nanocrystals), and cellulose microfibrils or nanofibrils can be extracted from wood pulp, plant fibers, sea animals, and certain bacteria.^[1–4] Due to their advantages, such as renewability, low cost, high specific stiffness and strength, low density, unique chemical and reactive surface properties, biodegradability, and biocompatibility, they have been used recently for the reinforcement of cellulose-based polymer composites, which have shown potential applications in fields such as biomedical and tissue engineering, enzyme immobilization, and so on.^[5–14]

MCC is basically crystalline cellulose derived from high-quality wood pulp and plant short fibers such as sisal fiber by acidic and alkaline treatment, and it is expected to disintegrate into cellulose whiskers after complete hydrolysis. Compared to conventional cellulose fibers, MCC, tens of microns in diameter and hundreds of microns in length, has high cellulose content, good crystallinity, and thermostability, where the lignin, hemicellulose, and amorphous regions are removed by alkaline treatment and acid hydrolysis. Therefore, MCC is a promising cellulosic reinforcing agent for polymer matrix. For example, Spoljaric et al.^[11] and Ashori et al.^[12] prepared an MCC-polypropylene (PP) composite, and the mechanical properties of the composites were significantly enhanced as compared to pure PP. Xiao et al.^[14] fabricated bio-based high-performance green composites from poly(lactic acid) (PLA) and MCC fibers grafted with L-lactic acid oligomers (g-MCC). The g-MC/PLA composites exhibit better mechanical properties than pure PLA, with a high tensile strength of 70 MPa, and a higher elongation at breakage. Similarly, Mathew et al.^[13] also fabricated biodegradable composites using MCC as the reinforcement and PLA as a matrix.

However, MCC, including plant short fibers and other cellulose solid particles, have poor compatibility with hydrophobic matrices and thermostability because of their natural instincts. These disadvantages result in poor adhesion to hydrophobic matrices, which can affect the mechanical properties and thermostability of the composites obtained. As a result, many attempts have been made to modify their surface to improve their compatibility with polymer matrix and thermostability by chemical cross-linking or grafting reaction.^[11,14–21] For example, isocyanate, N-acylureas, PEG, poly(styrene), and poly(*t*-butyl acrylate) were used to modify the surface of cellulose microcrystals (or nanocrystals, nanofibrils) in order to improve the compatibility with the polymer matrix or the dispersion in organic solvent.^[15–19] MCC was often treated with silicone oil, stearic acid, or alkyltitanate coupling agent to promote matrix-filler dispersion and compatibility.^[11] For example, MCC

grafted by L-lactic acid oligomer (g-MCC) had an improved compatibility with PLA, which also provided g-MCC/PLA composites with excellent transparency, as well as enhanced thermal and mechanical properties.^[14] Cunha et al.^[20] reported a heterogeneous chemical modification of cellulose fibers with (3-isocyanatopropyl) triethoxysilane, followed by the acid hydrolysis (and condensation) of the appended siloxane moieties, in the presence of either tetraethoxysilane or 1*H*,1*H*,2*H*,2*H*-perfluorodecyltriethoxysilane. These modifications produced an inorganic “coating” around the fibers and displayed a very pronounced hydrophobic and lipophobic character. In addition, montmorillonite nanoparticles and polyelectrolytes were adopted to modify the surface of lignocellulosic fibers by a layer-by-layer (LbL) assembly process in order to improve the thermostability.^[21] Sequeira et al.^[22] synthesized cellulose/silica hybrids (CSHs) by a sol-gel method using eucalyptus-bleached Kraft pulp as the cellulose source and tetraethyl orthosilicate (TEOS) as the silica precursor with heteropoly acids (HPAs) as catalysts. They pointed out that the hybrid materials showed considerably higher hydrophobicity (about four times) and thermal stability when compared to the starting fibrous material (bleached Kraft pulp). Barud et al.^[23] fabricated bacterial cellulose (BC)/silica hybrids from BC membranes and tetraethoxysilane (TEOS) under neutral pH conditions at rt. The thermal decomposition temperature of the BC/silica hybrids was improved compared to the pure BC.

In our previous work, sisal fibers as reinforcements were used to improve the mechanical properties, especially the tribological performance of polymer composites.^[24,25] In order to improve the compatibility of sisal fiber with polymer matrix, the sisal fibers were often treated with silane coupling agent or potassium permanganate.^[24–27] However, the thermostability of the composites was decreased because of the natural instincts of sisal fiber, especially due to the poor heat resistance of lignin and hemicellulose existing in sisal fibers. Thus, the problem to be solved for sisal fiber is how to improve the compatibility with the polymer matrix and especially the thermostability. Two schemes can be considered. On one hand, microcrystalline cellulose extracted from sisal fibers (SFMCC) can replace short sisal fibers as reinforcements to avoid the effect of lignin and hemicellulose components. On the other hand, depending on the reactive hydroxyl groups on their surface, SFMCC can be modified by a chemical agent, which can improve both the compatibility and thermostability of SFMCC.

Polyhedral oligomeric silsesquioxane (POSS) has a nanometer-sized confine structure with a cubic silica core and can be further functionalized with a variety of organic compounds. POSSs, as typical molecular nanobuilding blocks, can be effectively used to incorporate into and reinforce the polymer organic matrix by copolymerization, grafting, or even blending through traditional processing methods. The resulting nanocomposite showed improved mechanical properties and higher thermal stability, which is determined by

POSS/POSS and POSS/polymer interactions.^[28,29] For example, Wang et al.^[30] studied the thermal degradation behaviors of epoxy resin/octavinyl polyhedral oligomeric silsesquioxane (OVPOSS) hybrids and found that the incorporation of OVPOSS into epoxy resins obviously decreased the peak heat release rate and total heat release of the hybrids. The addition of OVPOSS retarded the oxidation of char residue and enhanced the flame resistance of epoxy resins. Xu et al.^[31] prepared a series of poly (4-acetoxystyrene) (PAS)/OVPOSS blends and polystyrene (PS)/OVPOSS blends by the solution-blending method. The results showed that OVPOSS can effectively improve the thermal stability of the PAS/POSS blends at low POSS content. The glass-transition temperature (T_g) of the PAS/POSS blends increases at a relatively low POSS content and then decreases at a relatively high POSS content. Xie et al.^[32] reported that POSSs were grafted onto cellulose fabrics by a chemical cross-linking reaction. They thought that POSS had also attracted considerable attention for heat-resistant paint and coatings due to the fact that thermal degradation of POSS leaves behind a “self-healing” SiO_2 layer.

In this article, SFMCC was fabricated and used to replace sisal short plants as reinforcements in our future work. Subsequently, octa-aminopropylsilsesquioxane (POSS-NH₂) nanoparticles were grafted on the surface of SFMCC by cross-linking graft reaction. Epichlorohydrin as a cross-linking agent was used in the graft reaction. The chemical and surface morphological structures of the organic/inorganic hybrids were characterized. The POSS/SFMCC hybrids had better thermostability than pure SFMCC, which could be used as reinforcements with good heat resistance and mechanical properties for fabrication of polymer composites. This work could also offer a method for the modification of MCC, including other cellulose solid particles.

RESULTS AND DISCUSSION

Morphology and Structure of SFMCC and POSS-NH₂ Nanoparticles

According to Morán,^[3] SFMCC can be extracted from sisal fibers by means of chemical procedures such as alkaline extraction, bleaching, and acid hydrolysis. The components of SFMCC can be concluded from the FTIR spectrum. From Figure 1, we can see that our SFMCC gave two main absorbance regions. The first one is at low wavelengths in the range 700–1800 cm^{-1} , and the second one is at higher wavelengths corresponding to the range of approximately 2700–3500 cm^{-1} . The bands at 3360 cm^{-1} and 2900 cm^{-1} correspond respectively to the stretching vibrations of O–H and H–C–H. The characteristic peaks of C–O–C in the cellulose glycopyranose ring were observed at 1170–1020 cm^{-1} . The band at 1726 cm^{-1} in the spectrum could be due to the presence of small amounts hemicellulose, which contains C=O linkage with

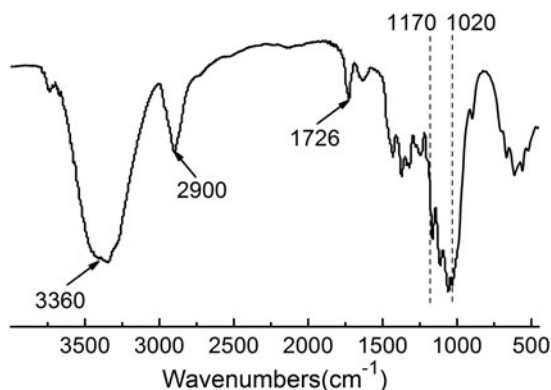


Figure 1: FTIR spectrum of microcrystalline cellulose extracted from sisal fibers (SFMCC).

the absorbance at $1765\text{--}1715\text{ cm}^{-1}$. Another possibility is that the carboxyl or aldehyde absorption (1728 cm^{-1}) could arise from the opened terminal glycopyranose rings or oxidation of the C–OH groups, and the 1726 cm^{-1} band corresponds to carbonyl groups. Thus, the presence of the band at 1726 cm^{-1} could be attributed to oxidation. When analyzing the spectra, it is evident that there was no remaining lignin in the obtained celluloses. This can be concluded from the absence of the absorption bands related to aromatic ring skeletal vibrations ($1500\text{--}1600\text{ cm}^{-1}$).^[3] Thus, the lignin and the majority of hemicelluloses had been removed from SFMCC, and the pure cellulose was obtained. Meanwhile, Figure 2a shows that SFMCC obtained was a white powder completely different from the short sisal fiber. The high-resolution morphology was further characterized by SEM, and the images with different magnifications are shown in Figures 2b and 2c. They clearly show that SFMCC had diameters of $10\text{--}20\text{ }\mu\text{m}$ and lengths of $50\text{--}150\text{ }\mu\text{m}$ and its surface was very neat.

Figure 3a is the AFM height image of the synthesized POSS-NH₂ nanoparticles, and Figure 3b is the height profile along the white line shown in

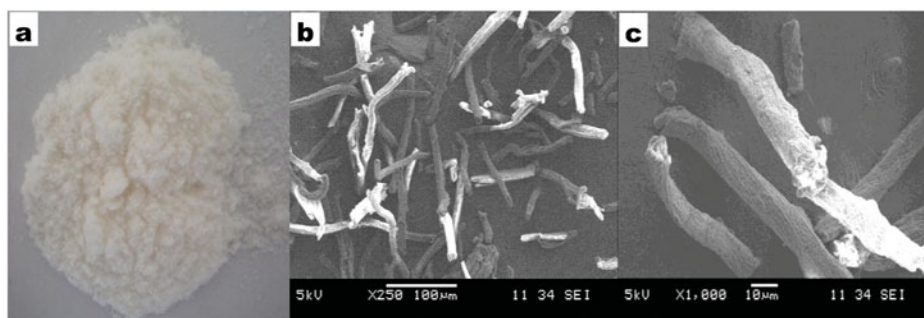


Figure 2: Photo (a) and SEM images (b, c) of SFMCC with different magnification.

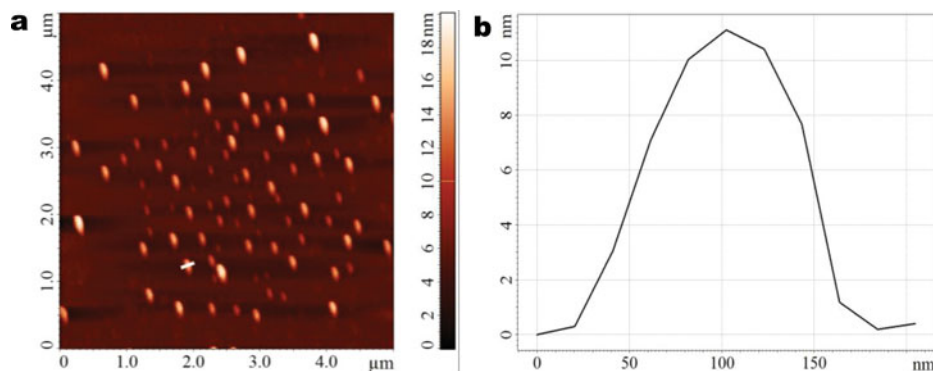


Figure 3: (a) AFM height image of the synthesized POSS-NH₂ nanoparticles and (b) height profile along the white line shown in (a).

Figure 3a. From Figure 3, we can conclude that POSS-NH₂ nanoparticles with diameters of several to 10 nanometers are well dispersed in CH₃OH solution. So, it is obvious that the size of POSS-NH₂ nanoparticles is far smaller than that of SFMCC.

Figure 4 is the FTIR spectrum of POSS-NH₂ nanoparticles. The wide and intensive band at 3360 cm⁻¹ is attributed to the characteristic absorption of NH₂ groups. The strong bands at 2930 and 2870 cm⁻¹ correspond to the C-H stretching of the CH₂ groups in the organic corner groups of the cage structure. The absorption band at 1130 cm⁻¹ is the characteristic vibration of the Si-O-Si bond. The absorption bands at 1030 cm⁻¹ are attributed to the characteristic vibrations of the silsesquioxane cage Si-O-Si framework. The band at 769 cm⁻¹ is the bending vibration of the Si-C bond in Si-CH₂.^[34] Therefore, the FTIR

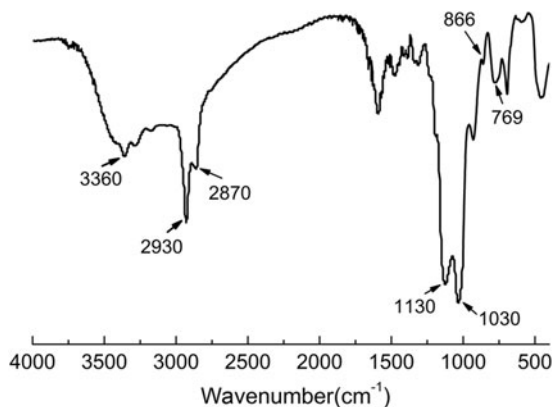


Figure 4: FTIR spectrum of POSS-NH₂ nanoparticles.

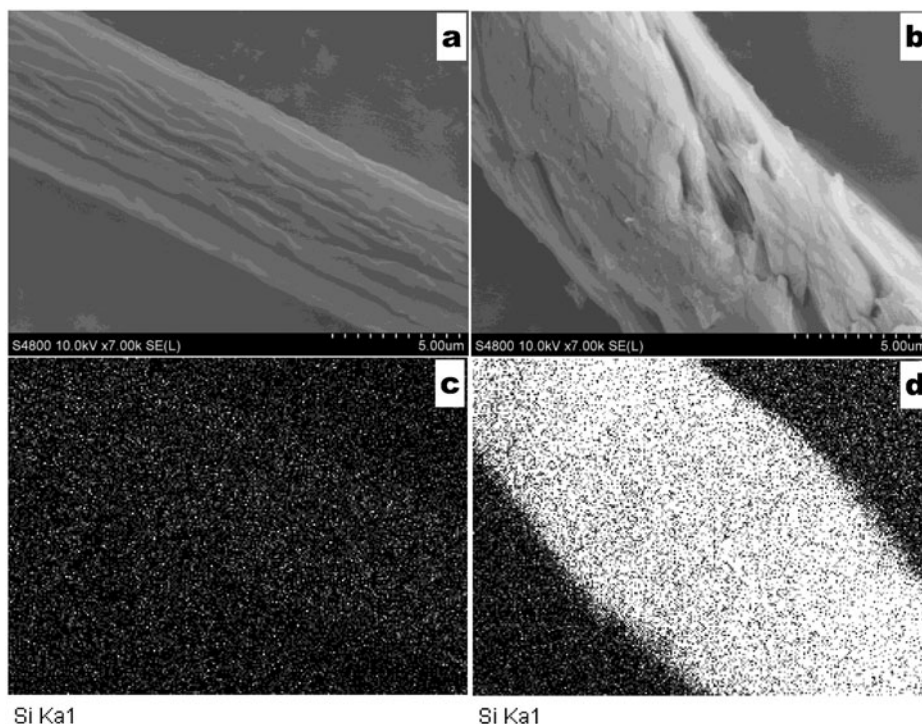


Figure 5: Two representative SEM/EDX analysis results of SFMCC and POSS/SFMCC hybrids: (a) and (b) are respectively the SEM images of SFMCC and POSS/SFMCC hybrids; (c) and (d) are the corresponding EDX mapping images.

spectrum of the product provided good assignment to the cage structure of POSS-NH₂.

Structure and Morphology of POSS/SFMCC Hybrids

In order to analyze the structure of POSS/SFMCC hybrids, FESEM equipped with an EDX elemental composition analyzer was used to characterize their surface structure and morphology. Figure 5 shows two representative SEM/EDX results of SFMCC and POSS/SFMCC hybrids. Figure 5a and 5b present respectively SEM images of SFMCC and POSS/SFMCC hybrids, while Figures 5c and 5d are the corresponding EDX mapping images. From Figures 5a and 5b, we can see that the surface of SFMCC is a little rough but regular, and the surface of POSS/SFMCC hybrids becomes irregular, probably because of the treatment of NaOH during the epoxidation of SFMCC. In the EDX mapping image of the silicon element of POSS/SFMCC hybrids (see Fig. 5d), the intensive bright spots representing silicon element display the same shape as shown in Figure 5b. It can be concluded that POSS-NH₂ nanoparticles had been grafted and homogeneously dispersed on the surface of SFMCC

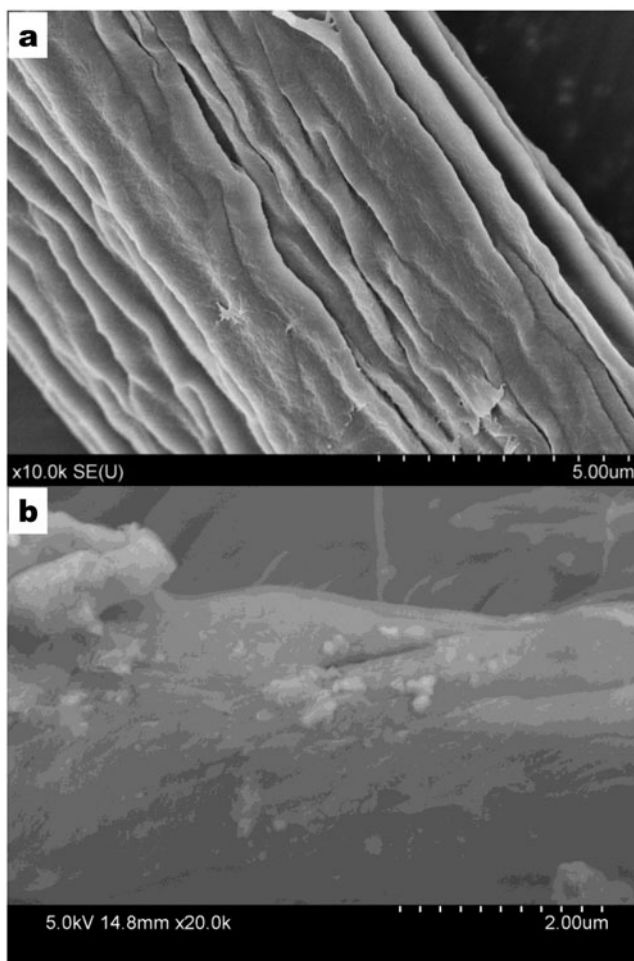


Figure 6: SEM images of SFMCC (a) and POSS/SFMCC hybrids (b).

matrix. Contrarily, there are not bright spots in the EDX mapping of the silicon element of SFMCC shown in Figure 5c, which showed that there was not a silicon element in SFMCC.

Figures 6a and 6b are respectively the SEM images of SFMCC and POSS/SFMCC hybrids in higher magnification. It can be seen that the surface of SFMCC is clean and regular. However, there are large numbers of white nanoparticles dispersed on the surface of POSS/SFMCC hybrids as shown in Figure 6b. These white nanoparticles are about tens of nanometers in diameter larger than the size of POSS-NH₂ nanoparticles, which may result from the aggregation of POSS-NH₂ nanoparticles during the grafting reaction. Thus, we can conclude that the POSS-NH₂ nanoparticles have been successfully grafted on the surface of SFMCC.

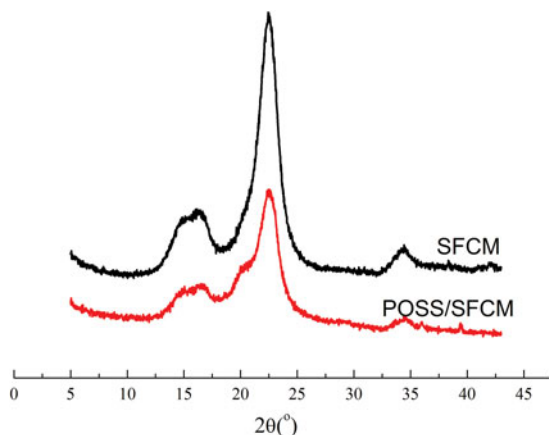


Figure 7: XRD patterns of SFMCC and POSS/SFMCC hybrids.

The XRD data illustrate the influence of POSS-NH₂ nanoparticles on the intensity and shape of the patterns. POSS-NH₂ has typical nano-SiO₂ crystals. X-ray patterns of POSS-NH₂ feature main peaks at 7.06° and 21.32° associated with the nano-SiO₂ crystal structure. XRD patterns of SFMCC and POSS/SFMCC hybrids are shown in Figure 7. The main peaks of POSS/SFMCC hybrids at 14.89°, 16.27°, and 22.58° are associated with cellulose structure. Many researchers reported that POSS could crystallize when they were copolymerized with polymers.^[36] So, in the XRD patterns of POSS/SFMCC hybrids, there is a weak diffraction peak at 21.51°, which is associated with the main peak of POSS-NH₂ at 21.32°. However, the peak of POSS-NH₂ at 7.06° was not observed, which can be explained by the fact that the peak at 7.06° associated with the nano-SiO₂ structure may be overlapped.^[32] Meanwhile, it can be noticed that SFMCC is presented in the form of cellulose I, rather than cellulose II, which arises from the fact that there is no doublet in the intensity of the main peak.^[37] The crystallinity index (I_c) can be determined by using the following equation:^[38]

$$I_c = \frac{(I_{(002)} - I_{(am)})}{I_{(002)}} \times 100$$

where $I_{(002)}$ is the counter reading at peak intensity at a 2θ angle close to 22°, representing crystalline material, and $I_{(am)}$ is the counter reading at peak intensity at a 2θ angle close to 16°, representing amorphous material in cellulosic fibers. The results show that the crystallinity is similar for SFMCC and POSS/SFMCC (Crystallinity Index $I_c = 71 \pm 1$). It can be concluded that the addition of POSS-NH₂ nanoparticles has no influence on the crystallinity of POSS/SFMCC hybrids. One possible reason is that the grafting reaction on the surface of SFMCC did not damage the crystal structure of SFMCC, and

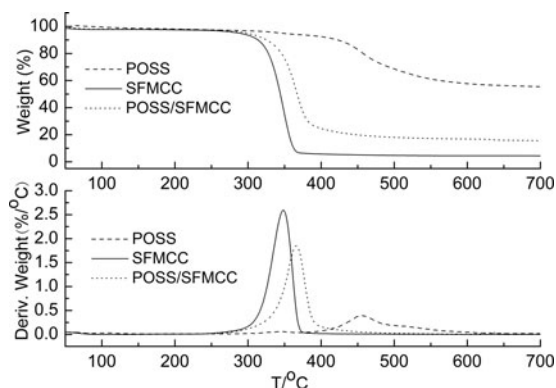


Figure 8: TGA (upper) and DTG (lower) curves of POSS, SFMCC, and POSS/SFMCC hybrids.

another possible reason is that the weight of POSS-NH₂ nanoparticles grafting onto the surface of SFMCC is not high enough to overlap the XRD patterns of SFMCC.

Thermal Properties of POSS/SFMCC Hybrids

The thermal properties of POSS/SFMCC hybrids are different from that of SFMCC. Thermogravimetric analysis (TGA) and differential scanning calorimetry (DSC) are usually used to study the thermal characteristics of materials. Figure 8 shows the TGA (upper) and DTA (Differential Thermal Analysis) (down) curves of POSS, SFMCC, and POSS/SFMCC hybrids, and characteristic parameters from TGA data are presented in Table 1. DSC plots of SFMCC and POSS/SFMCC hybrids are shown in Figure 9.

From Figure 8 and Table 1, we can see that POSS/SFMCC hybrids had a sharp weight loss starting at 342°C, which was higher than SFMCC starting at 326°C, and stopped pyrolyzing at 384°C, which was also higher than SFMCC, stopping at 361°C. The maximum thermal decomposition temperature for POSS/SFMCC hybrids was 367°C, compared to 348°C of SFMCC. The residual mass of POSS/SFMCC hybrids and SFMCC are 15.6 wt% and 4.4wt%

Table 1: Characteristic parameters from TGA data of POSS, SFMCC, and POSS/SFMCC hybrids

	$T_{\text{Onset}}/^{\circ}\text{C}$	$T_{\text{End}}/^{\circ}\text{C}$	$T_{\text{inflection}}/^{\circ}\text{C}$	Residual mass (%)
SFMCC	326	361	348	4.4
POSS/SFMCC	342	384	367	15.6
POSS	398	522	449	56.5

at 700°C, respectively. Clearly, compared to SFMCC, POSS/SFMCC hybrids had higher decomposition temperature and more residual mass. We can conclude that the thermal properties of SFMCC were improved upon POSS grafting onto its surface. It can be explained by the fact that the Si–C and Si–O bond energy in molecular POSS are higher than the C–C bond energy, and POSS nanoparticles that accumulated on the surface of SFMCC by a chemical grafting reaction can form an inorganic protective layer to decrease SFMCC decomposition. On the other hand, POSS nanoparticles bonded to SFMCC can restrict the macromolecular segment movement of SFMCC at high temperature, which can increase the heat resistance of SFMCC. This can further be evidenced by the SEM images of SFMCC and POSS/SFMCC after being charred in N₂ at 700°C, which are shown in Figure 10. From Figure 10, it is clear that after being charred, the diameter of SFMCC obviously shrunk and helical structures appeared on the surface. However, the appearance of POSS/SFMCC hybrids before and after being charred has no obvious difference. It further proved that POSS nanoparticles in hybrids can protect SFMCC during heating and prevent them from decomposition. In short, the thermal properties of SFMCC can be improved by introducing POSS nanoparticles onto its surface.

In addition, further analysis of the DTA data of POSS, SFMCC, and POSS/SFMCC hybrids showed that the weight ratio of POSS in hybrids is calculated at about 22%. Then, the weight of POSS is about 28% of SFMCC in hybrids. According to the reaction formula of ep-SFMCC and POSS-NH₂, the theoretical graft weight of POSS is 114% of ep-SFMCC calculated from the epoxy value, 0.14 mol/100 g, of the obtained ep-SFMCC. So it can be said that the grafting efficiency of POSS on the surface ep-SFMCC is about 25%, where the grafting efficiency is defined as the ratio of weight of POSS actually involved in the graft reaction and the theoretical graft weight of POSS. One

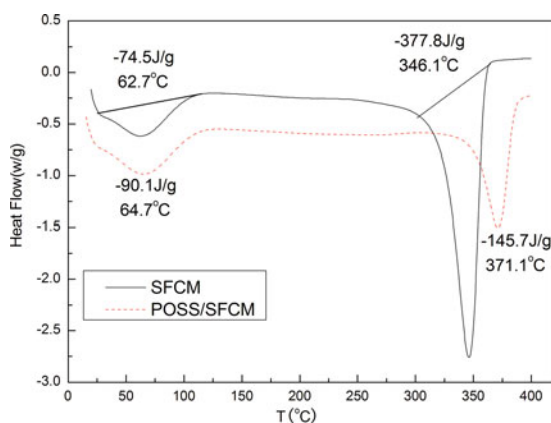


Figure 9: DSC plots of SFMCC (solid) and POSS/SFMCC hybrids (dashed).

possible reason is the accessibility of solid phase reaction between POSS-NH₂ nanoparticles, and ep-SFMCC, and the other reason is a steric effect because of the much larger molecular size of POSS-NH₂ than the epoxy group.

The DSC plots for SFMCC and POSS/SFMCC hybrids contain first endothermic peaks at 62.7°C and 64.7°C, respectively. These endothermic peaks are probably associated with the removal of water from the SFMCC and POSS/SFMCC hybrids. For SFMCC, the second endothermic peak at 346.1°C is close to the maximum thermal decomposition temperature of SFMCC. The endothermic change is associated with SFMCC decomposition during heating, and there was no enthalpy change before decomposition of SFMCC because of the higher melting temperature than decomposition temperature of SFMCC. For POSS/SFMCC hybrids, the second endothermic peak at 371.1°C is also close to the maximum thermal decomposition temperature of POSS/SFMCC hybrids. The endothermic change may be associated with the decomposition of POSS/SFMCC hybrids during heating. Moreover, the endothermic peaks become small. It indicates that the decomposition might take place in the organic phase. This phenomenon also showed that POSS nanoparticles in the hybrids could protect SFMCC and prevent them from decomposition during heating.

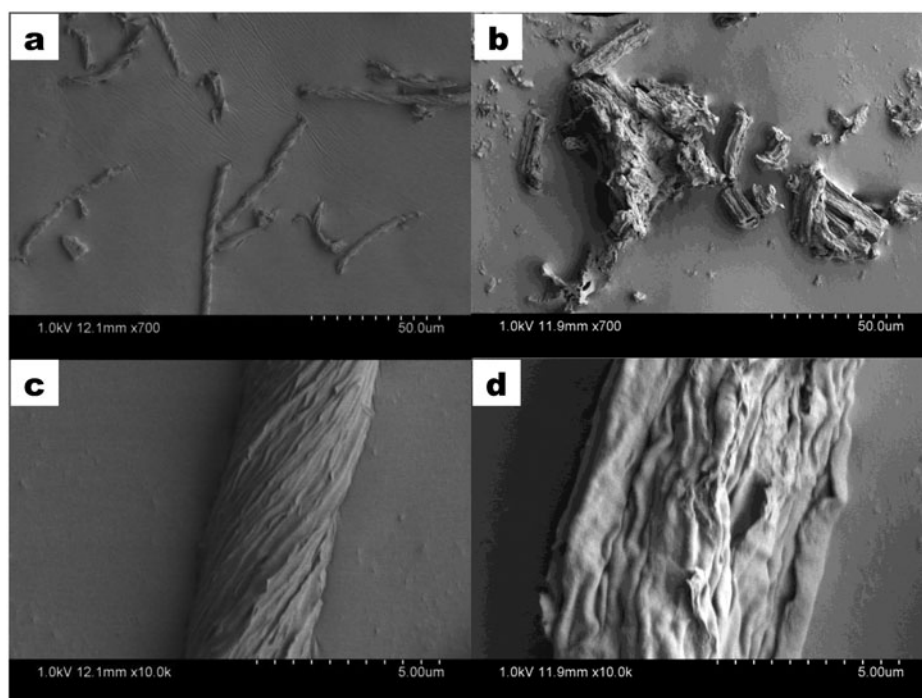
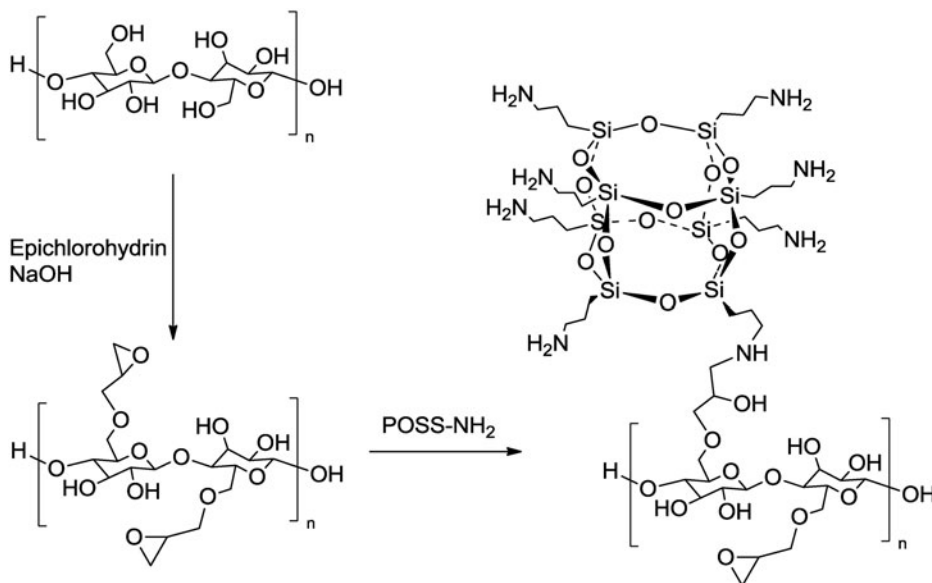


Figure 10: SEM images of SFMCC and POSS/SFMCC hybrids after being charred in N₂ at 700°C.

Thus, the thermal properties of SFMCC were improved by introducing POSS nanoparticles onto its surface.



Scheme 1: The illustration of reaction process of POSS-NH₂ and SFMCC.

CONCLUSIONS

POSS/SFMCC hybrids were successfully fabricated through a simple cross-linking graft reaction where epichlorohydrin was used as the cross-linking reagent. The chemical structure and morphology of POSS-NH₂ nanoparticles, SFMCC, and POSS/SFMCC hybrids were characterized by FTIR spectra, X-ray diffraction, AFM, and SEM. The results showed that SFMCC, with diameters of 10–20 μm and lengths of 50–150 μm , was pure cellulose without lignin and hemicelluloses. The obtained POSS-NH₂ nanoparticles had diameters of several to 10 nanometers. POSS-NH₂ nanoparticles could be grafted onto the surface of SFMCC, forming novel macromolecular structures coated by POSS nano-silica particles. POSS particles are dispersed at nanometer scale in the cellulose host matrix, bonding to the cellulose through covalent bonds. The results of TGA and DSC demonstrated that POSS/SFMCC hybrids had higher decomposition temperature, more residual mass, and less endothermic change, which proved that POSS nanoparticles in the hybrids could protect SFMCC under heating conditions and prevented them from decomposition, and that the thermal properties of SFMCC were improved by grafting POSS onto its surface.

EXPERIMENTAL

Materials

Sisal fibers were supplied by Guangxi Sisal Company. Epichlorohydrin (EPC, 99.5%), γ -aminopropyltriethoxysilane (KH550, 99%), tetrahydrofuran, hydrochloric acid, acetone, and sulfuric acid were purchased from Aladdin Chemistry Co. Ltd. (Shanghai, China) and used directly.

Synthesis of Octa-Aminopropyl Polyhedral Oligomeric Silsesquioxane (POSS-NH₂) Nanoparticles

The process for the synthesis of octa-aminopropyl polyhedral oligomeric silsesquioxane (POSS-NH₂) followed a modified method of Feher and Zhang.^[33,34] KH550 (20.13 g) was added in a three-necked round-bottomed flask with continuous stirring. Then, a mixture of 59.5 g of tetrahydrofuran and 14.21 g of distilled water was added dropwise. Subsequently, the temperature was raised up to 60°C and several drops of hydrochloric acid were added. After 72 h, a white precipitate was obtained by adding equal volume of tetrahydrofuran into the reaction solution. The precipitate product was filtered off, washed with tetrahydrofuran, and dried at 40°C in a vacuum oven for 24 h.

Extraction of Microcrystalline Cellulose From Sisal Fibers

As-received sisal fibers were preconditioned before cellulose extraction took place; the fibers were washed with distilled water several times and dried in an oven at 80°C for 24 h. Then, they were chopped to an approximate length of 4 mm. The extraction of microcrystalline cellulose from sisal fibers was performed according to the method by Morán.^[3] Finally, SFMCC as a white powder was obtained.

Fabrication of POSS/SFMCC Hybrids

The surface of SFMCC was decorated with epoxy functional groups via reaction with epichlorohydrin (4 mL/g cellulose) in 1 M sodium hydroxide (100 mL/g cellulose) according to the method by Dong and Roman.^[35] After 2 h of reaction at 60°C, the reaction mixture was centrifuged and washed with distilled water multiple times until epichlorohydrin was washed off completely. The content of epichlorohydrin in the washing solution was determined using sodium thiosulfate and phenolphthalein as indicator. Finally, the product, marked as ep-SFMCC, was obtained after being dried in a vacuum oven at 60°C. The epoxy value of the final product is measured as 0.14 mol/100 g by the conductometric titration method.

ep-SFMCC (0.2 g) and distilled water (60 mL) were mixed and added in a three-neck flask equipped with reflux condenser with continuous stirring. After the temperature was raised to 80°C, 40 mL of distilled water containing 0.630 g of POSS-NH₂ was added into the flask dropwise in 30 min through a dropping funnel. Then, 1 mL of 95% ethanol was added, and the reaction was kept at 100°C for 1.5 h. Finally, the product was washed with distilled water until the redundant POSS-NH₂ was washed off completely, and dried in a vacuum oven at 60°C for 12 h. The whole crosslinking reaction of POSS-NH₂ and SFMCC was illustrated in Scheme 1.

Characterization

The AFM image was obtained with NT-MDT SPM (Russia) at rt, in tapping mode. The sample was obtained by dropping the dispersion of POSS-NH₂ nanoparticles in CH₃OH onto a mica sheet and dried in a vacuum at 40°C for 12 h. The FT-IR spectra were recorded as KBr pellets on a NICOLET NEXUS 470 infrared spectrometer (America) in the transmission mode from 400 to 4000 cm⁻¹ with a 2 cm⁻¹ resolution. For SEM analysis, the dried samples were sputtered with gold and then examined with an S-4800 FE-SEM machine (Hitachi High-Technologies Corporation, Japan), operated at 10 kv. Elemental mapping of the samples was identified by energy-dispersive X-ray analysis (EDXA, Model: Oxford Instruments), which was coupled by SEM. The XRD was measured with a PANalytical B.V.X/Pert PRO X-Ray diffractometer, which used a Cu-K target at 40 kV, 300 mA, $\lambda = 1.542 \text{ \AA}$. Samples were scanned in 2θ ranges varying from 5° to 40° (1°/min). TGA of SFMCC and POSS/SFMCC hybrids was assessed on a Netzsch STA-449 instrument with a heating rate of 10°C/min in an N₂ flow. DSC was measured with a Netzsch DSC-204 instrument using indium standards for calibration with a heating rate of 5°C/min from 20°C to 400°C. N₂ (20 mL/min) was employed as the purge gas for the sample and reference cells.

FUNDING

The authors would like to acknowledge the National Natural Science Foundation of China (No. 21264005, No. 21204013); Guangxi Natural Science Foundation (No. 2012GXNSFBA053153, No. 2013GXNSFDA019008); Foundation of Guangxi Scientific Experiment Center of Mining, Metallurgy and Environment (No. KH2012YB001); Guangxi Small Highland Innovation Team of Talents in Colleges and Universities; and Guangxi Funds for Specially-appointed Expert.

REFERENCES

1. Teixeira, E.M.; Corre a, A.C.; Manzoli, A.; Leite F.L.; Oliveira, C.R.; Mattoso, L.H.C. Cellulose nanofibers from white and naturally colored cotton fibers. *Cellulose* **2010**, *17*, 595–606.
2. Fukuzumi, H.; Saito, T.; Iwata, T.; Kumamoto, Y.; Isogai, A. Transparent and high gas barrier films of cellulose nanofibers prepared by TEMPO-mediated oxidation. *Biomacromolecules* **2009**, *10*, 162–165.
3. Mor n, J.I.; Alvarez, V.A.; Cyras, V.P.; V zquez, A. Extraction of cellulose and preparation of nanocellulose from sisal fibers. *Cellulose* **2008**, *15*, 149–159.
4. Iguchi, M.; Yamanaka, S.; Budhiono, A. Bacterial cellulose—a masterpiece of nature’s arts. *J. Mater. Sci.* **2000**, *35*, 261–270.
5. Siqueira, G.; Bras, J.; Dufresne, A. Cellulose whiskers versus microfibrils: influence of the nature of the nanoparticle and its surface functionalization on the thermal and mechanical properties of nanocomposites. *Biomacromolecules* **2009**, *10*, 425–432.
6. Lee, J.; Deng, Y. Increased mechanical properties of aligned and isotropic electrospun PVA nanofiber webs by cellulose nanowhisiker reinforcement. *Macromol. Res.* **2012**, *20*, 76–83.
7. Liu, D.; Yuan, X.; Bhattacharyya, D. The effects of cellulose nanowhiskers on electrospun poly (lactic acid) nanofibres. *J. Mater. Sci.* **2012**, *47*, 3159–3165.
8. Liu, H.; Laborie, M.G. Bio-based nanocomposites by in situ cure of phenolic prepolymers with cellulose whiskers. *Cellulose* **2011**, *18*, 619–630.
9. Nakagaito, A.N.; Yano, H. The effect of fiber content on the mechanical and thermal expansion properties of biocomposites based on microfibrillated cellulose. *Cellulose* **2008**, *15*, 555–559.
10. Spoljaric, S.; Genovese, A.; Shanks, R.A. Polypropylene-microcrystalline cellulose composites with enhanced compatibility and properties. *Compos. Part A-Appl. S.* **2009**, *40*, 791–799.
11. Ashori, A.; Nourbakhsh, A. Performance properties of microcrystalline cellulose as a reinforcing agent in wood plastic composites. *Compos. Part B-Eng.* **2010**, *41*, 578–581.
12. Mahmoud, K.A.; Male, K.B.; Hrapovic, S.; Luong, J.H.T. Cellulose nanocrystal/gold nanoparticle composite as a matrix for enzyme immobilization. *ACS Appl. Mater. Inter.* **2009**, *1*, 1383–1386.
13. Mathew, A.P.; Oksman, K.; Sain, M. Mechanical properties of biodegradable composites from poly lactic acid (PLA) and microcrystalline cellulose (MCC). *J. Appl. Polym. Sci.* **2005**, *97*, 2014–2025.
14. Xiao, L.; Mai, Y.; He, F.; Yu, L.; Zhang, L.; Tang, H.; Yang, G. Bio-based green composites with high performance from poly(lactic acid) and surface-modified microcrystalline cellulose. *J. Mater. Chem.* **2012**, *22*, 15732–15739.
15. Siqueira, G.; Bras, J.; Dufresne, A. New process of chemical grafting of cellulose nanoparticles with a long chain isocyanate. *Langmuir* **2009**, *26*, 402–411.
16. Giron s, J.; Pimenta, M. T. B.; Vilaseca, F.; de Carvalho, A. J. F.; Mutj , P.; Curvelo, A. A. S. Blocked isocyanates as coupling agents for cellulose-based composites. *Carbohydr. Polym.* **2007**, *68*, 537–543.
17. Fujisawa, S.; Okita, Y.; Saito, T.; Togawa, E.; Isogai, A. Formation of N-acylureas on the surface of TEMPO oxidized cellulose nanofibril with carbodiimide in DMF. *Cellulose* **2011**, *18*, 1191–1199.

18. Araki, J.; Wada, M.; Kuga, S. Steric stabilization of a cellulose microcrystal suspension by poly (ethylene glycol) grafting. *Langmuir* **2001**, *17*, 21–27.
19. Thielemans, W.; Belgacem, M. N.; Dufresne, A. Starch nanocrystals with large chain surface modifications. *Langmuir* **2006**, *22*, 4804–4810.
20. Cunha, A. G.; Freire, C. S. R.; Silvestre, A. J. D.; Neto, C. P.; Gandini, A. Preparation and characterization of novel highly omniphobic cellulose fibers organic-inorganic hybrid materials. *Carbohydr. Polym.* **2010**, *80*, 1048–1056.
21. Lin, Z.; Renneckar, S.; Hindman, D. P. Nanocomposite-based lignocellulosic fibers 1. Thermal stability of modified fibers with clay-polyelectrolyte multilayers. *Cellulose* **2008**, *15*, 333–346.
22. Sequeira, S.; Evtuguin, D. V.; Portugal, I.; Esculcas, A. P. Synthesis and characterisation of cellulose/silica hybrids obtained by heteropoly acid catalysed sol-gel process. *Mat. Sci. Eng. C* **2007**, *27*, 172–179.
23. Barud, H. S.; Assunção, R. M. N.; Martines, M. A. U.; Dexpert-Ghys, J.; Marques, R. F. C.; Messaddeq, Y. Bacterial cellulose-silica organic-inorganic hybrids. *J. Sol-Gel Sci. Techn.* **2008**, *46*, 363–367.
24. Mu, Q.; Wei, C.; Feng, S. Studies on mechanical properties of sisal fiber/phenol formaldehyde resin in-situ composites. *Polym. Composite.* **2009**, *30*, 131–137.
25. Xiong, X.; Wei, C.; Zeng, M. Study on the tribological performance of sisal fiber/polysulfone/phenolic composite friction material. *Adv. Sci. Lett.* **2011**, *4*, 1108–1112.
26. Patra, A.; Bisoyi, D.; Manda, P. Electrical and mechanical properties of the potassium permanganate treated short sisal fiber reinforced epoxy composite in correlation to the macromolecular structure of the reinforced fiber. *J. Appl. Polym. Sci.* **2013**, *128*, 1011–1019.
27. Jiang, A.; Xi, J.; Wu, H. Effect of surface treatment on the morphology of sisal fibers in sisal/polylactic acid composites. *J. Reinf. Plast. Comp.* **2012**, *31*, 621–630.
28. Strachota, A.; Kroutilová, I.; Kovářová, J.; Matějka, L. Epoxy networks reinforced with polyhedral oligomeric silsesquioxanes (POSS). Thermomechanical properties. *Macromolecules* **2004**, *37*, 9457–9464.
29. Ramírez, C.; Rico, M.; Torres, A.; Barral, L.; López, J.; Montero, B. Epoxy/POSS organic-inorganic hybrids: ATR-FTIR and DSC studies. *Eur. Polym. J.* **2008**, *44*, 3035–3045.
30. Wang, X.; Hu, Y.; Song, L.; Xing, W. Y.; Lu, H. D. Thermal degradation behaviors of epoxy resin/POSS hybrids and phosphorus-silicon synergism of flame retardancy. *J. Polym. Sci. Part B: Polym. Phys.* **2010**, *48*, 693–705.
31. Feng, Y.; Jia, Y.; Guang, S. Y.; Xu, H. Y. Study on thermal enhancement mechanism of POSS-containing hybrid nanocomposites and relationship between thermal properties and their molecular structure. *J. Appl. Polym. Sci.* **2010**, *115*, 2212–2220.
32. Xie, K.; Zhang, Y.; Yu, Y. Preparation and characterization of cellulose hybrids grafted with the polyhedral oligomeric silsesquioxanes (POSS). *Carbohydr. Polym.* **2009**, *77*, 858–862.
33. Feher, F. J.; Wyndham, K. D. Amine and ester-substituted silsesquioxanes: synthesis, characterization and use as a core for starburst dendrimers. *Chem. Commun.* **1998**, 323–324.
34. Zhang, Z.; Liang, G.; Lu, T. Synthesis and characterization of cage Octa(aminopropylsilsesquioxane). *J. Appl. Polym. Sci.* **2007**, *103*, 2608–2614.

35. Dong, S.; Roman, M. Fluorescently labeled cellulose nanocrystals for bioimaging applications. *J. Am. Chem. Soc.* **2007**, *129*, 13810–13811.
36. Ohno, T.; Tagawa, S.; Itoh, H.; Suzuki, H.; Matsuda, T. Size effect of TiO₂-SiO₂ nano-hybrid particle. *Mater. Chem. Phys.* **2009**, *113*, 119–123.
37. Deraman, M.; Zakaria, S.; Murshidi, J. A. Estimation of crystallinity and crystallite size of cellulose in benzylated fibres of oil palm empty fruit bunches by X-Ray diffraction. *J. Appl. Phys.* **2001**, *40*, 311–315.
38. Mwaikambo, L. Y.; Ansell, M. P. Chemical modification of hemp, sisal, jute, and kapok fibers by alkalization. *J. Appl. Polym. Sci.* **2002**, *84*, 2222–2234.